

# Optimising the readout process in integrated phase-change photonic memory and computing devices

J. Song<sup>1\*</sup>, J. Pady<sup>1</sup>, N. Farmakidis<sup>2</sup>, H. Bhaskaran<sup>2</sup>, W.H.P. Pernice<sup>3,4</sup> and C. D. Wright<sup>1</sup>

<sup>1</sup>Centre for Metamaterial Research and Innovation, University of Exeter, UK

<sup>2</sup>Department of Materials, University of Oxford, Oxford OX1 3PH, UK

<sup>3</sup>Institute of Physics, University of Münster, Heisenbergstr. 11, 48149 Münster, Germany

<sup>4</sup>Kirchhoff-Institute for Physics, Heidelberg University, Im Neuenheimer Feld 227, 69120, Germany

\*Corresponding author: J.Song2@exeter.ac.uk

## ABSTRACT

In integrated phase-change photonic memory and computing devices, the basic operation involves using light guided into an integrated waveguide to switch the phase-change cell between its crystalline and amorphous states. Such switching results in a non-volatile and reversible alteration of the waveguide's optical transmission, thus forming the basis of the readout process. In terms of detecting the readout signal, a high signal-to-noise ratio (SNR) is obviously desirable. Optimising readout SNR involves a trade-off between readout contrast and insertion loss. Here we explore role of cell size and the size of the written mark on the readout signal, developing a realistic figure-of-merit to help guide design choices and deliver an optimum readout signal.

**Keywords** : Phase-change photonic memory, Multiphysics modelling.

## 1. INTRODUCTION

Integrated phase-change photonic memory devices offer a novel route to non-volatile storage and computing. Such devices generally consist of integrated waveguide structures onto which are fabricated small phase-change memory cells (using e.g.  $\text{Ge}_2\text{Sb}_2\text{Te}_5$  (GST)). When combined with photonic crossbar arrays and microring resonators, such photonic phase-change devices can deliver non-von Neumann forms of in-memory and neuromorphic photonic computing [1,2].

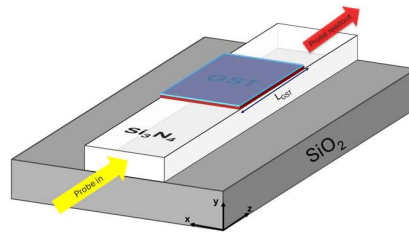


**Fig. 1.** Integrated phase-change photonic memory, configuration and operation schematic.

Here, we consider the evanescent-field coupling and power(heat) transfer between a GST cell and the propagating optical mode within a  $\text{Si}_3\text{N}_4$  waveguide operating at 1550 nm wavelength with 10 nm GST capped with 5 nm indium-tin oxide (ITO) to avoid oxidation, as shown in Fig. 1. The propagating optical mode in the waveguide is specified as the TE mode. For simulation of the phase-change process, i.e., writing and erasing (amorphization and recrystallization) of the GST cell, a model is used that combines thermo-optic finite-element simulations (using COMSOL Multiphysics) with a “bespoke” phase-change model [3] based on a Gillespie-type cellular automata and classical nucleation and growth theory.

## 2. RESULTS & DISCUSSION

For the *write* process, i.e. the writing of an amorphous mark into a fully crystalline starting state, a single 10 mW, 25 ns pulse with 2.5 ns rise/fall time is delivered along the waveguide. Simulated

microstructure within the GST cell is shown in Fig. 2(a), for a range of GST cell lengths. It can be seen that the amorphous mark is located at the front edge of the cell, and that the proportion of the cell that is switched depends on the cell size. The latter observation is confirmed in Fig. 2(b), which shows the crystal fraction ( $X$ ) before, during and after the writing pulse. For a 1.2  $\mu\text{m}$  GST cell, initially the cell is fully crystalline ( $X = 1$ ), with the crystalline fraction beginning to reduce at 4 ns and settling at a value of  $X \approx 0.7$  directly after the end of the write pulse. The change of the fraction of crystallized material in the cell leads to a corresponding change in optical transmission through the waveguide, leading to an increase in readout contrast, as shown in Fig. 3(a).

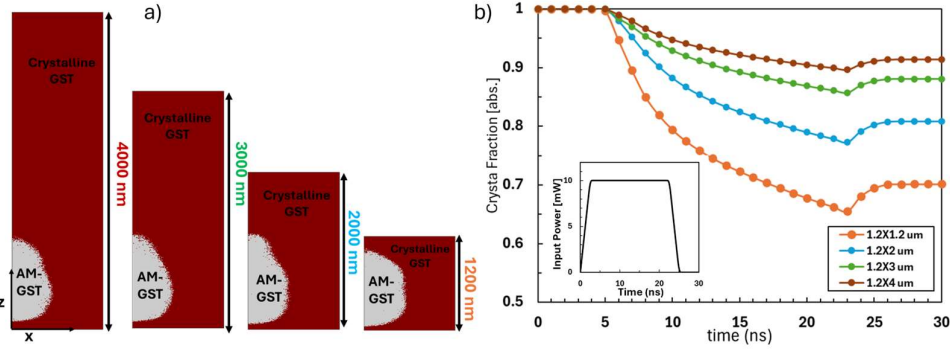


**Fig. 2.** (a) Top view of the microstructures of GST patch after write (amorphization) operations of the device with a function of GST lengths. (b) Simulated crystal fraction as a function of GST lengths.

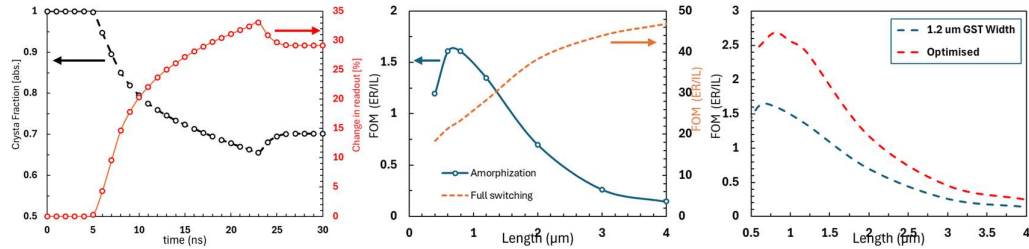


**Fig. 3.** (a) Crystal fraction, readout contrast during write process of the device with a 1.2  $\mu\text{m}$  long GST patch. (b) Figure of Merit (FOM) of the device as a function of GST patch length. (c) FOM of optimized devices.

The optimal size of the GST cell should maximize the readout figure of merit (FOM) of the device that relates the insertion loss (IL) and the extinction ratio (ER), i.e.,  $\text{FOM} = \text{ER}/\text{IL}$ . The readout FOM for GST cells of lengths ranging from 0.6 to 4  $\mu\text{m}$  is shown (blue solid line) in Fig. 3(b). In general the FOM increases with decreasing cell length, reflecting the variation of the crystallization fraction with cell length as a result of the writing process. A peak FOM of around 1.6 is observed for a cell length approximately 0.8  $\mu\text{m}$ . Note that these FOM values are lower than those previously reported in [4] (see red dashed line in 3(b)), since in that work it was assumed, unrealistically, that the entire cell can be switched between amorphous and crystalline states. While increasing the optical write power can increase the sizes of the written amorphous mark, powers above around 15 mW lead to damaging temperatures in the cell approaching 2000 K. Finally, we note that further optimisation of the FOM can be achieved by suitable alterations to the GST cell shape, with example results in Fig. 3(c).

The authors acknowledge funding via the H2020 project PHOENICS (Grant No. 101017237) and the EPSRC grant EP/W022931/1.

## REFERENCES

1. J. Feldmann et al., *Nature*, volume 569, pages 208-214, 2019
2. J. Feldmann et al., *Nature*, volume 589, pages 52-58, 2021
3. J. Pady et al., *Phys Status Solidi RRL*, 2300425, 2024.
4. J. Parra et al., *Scientific Reports*, volume 12, 9774, 2022.